A MICRO TURBINE DEVICE WITH ENHANCED MICRO AIR-BEARINGS

X.-C. Shan, Qide Zhang, Y.F. Sun, R. Maeda

DTIP of MEMS & MOEMS Stresa, Italy, 26-28 April 2006

A MICRO TURBINE DEVICE WITH ENHANCED MICRO AIR BEARINGS

X. C. Shan [1], Q. D. Zhang [2], Y. F. Sun[1] and R. Maeda [3]

[1] Singapore Institute of Manufacturing Technology, Singapore 638075
[2] Data Storage Institute, 5 Engineering Drive 1, Singapore 117608
[3] MEMS & Packaging Lab, AIST, Namiki 1-2, Tsukuba, 305-8564 Japan

ABSTRACT

As part of progress in developing a micro gas turbine engine, this paper presents the design, fabrication and testing of a silicon-based micro turbine device, which is driven by compressed air. To improve its rotational speed and stability, the turbine device has enhanced journal air bearing and thrust air bearings. The thrust air bearings are utilized for supporting the rotor from both its top- and bottom- sides. The top thrust air bearing employs pump-in type spiral grooves, and the bottom bearing uses pump-out type grooves. The journal air bearing is a plain journal with a critical short journal length (*L*) and a small radial clearance (*C*). Aspect ratio (*L:C*) above 20:1 is realized using optimized DRIE process. The micro turbine device has been fabricated and tested. The turbine device can sustain stable operations, and a rotation speed of 15,000 rpm has been reported during test.

1. INTRODUCTION

Micro gas turbine engine [1-2] is one of the promising solutions to provide high-density power source for microsystems. We are developing a silicon-based micro gas turbine engine [3], which consists of a combustor, a radial inflow turbine and a centrifugal compressor. A micro combustor composed of seven layers of silicon structures has been developed, which can sustain a stable combustion with an exit temperature as high as 1600 K [3]. The micro turbine is another critical component in micro gas turbine engine, which will generate power output and drive the compressor.

The critical concerns for a turbine device are friction and wear during operation. Micro air bearing is preferred in microsystems due to its miniaturized dimension and capability to achieve high speed and low wear operations. Some researchers have employed micro air bearings into rotational microsystems [4-6].

A conventional rotor has a dimension of a few millimeters along its axial direction. However, the rotor in a silicon-based micro turbine has an axial dimension (*L*) of less than one millimeter and a diameter (*D*) of several millimeters. The commonly accepted assumptions and design rules for conventional air bearings need to be revised due to the consequences of scaling down as well as the current limitations in micro fabrication techniques. Piekos [7] has investigated the performance of a short journal bearing in micro turbine system. A categorization of non-dimensional variables was suggested including loading and fluid.

This paper reports on design, fabrication and testing of a silicon-based micro turbine device. The turbine device consists of dynamic journal bearing and thrust air bearings, which are designed based on numerical simulation and fabricated through DRIE process. The turbine is driven by compressed air instead of exhausted gas from a micro combustor during test. Experimental investigations demonstrate that stable operations can be sustained, and a rotation speed of 15,000 rpm has been achieved.

2. DESIGN OF MICRO TURBINE STRUCTURE

The turbine device to be developed consists of three layers of silicon dies and two acrylic plates for tubing and clamping. Fig. 1 shows the schematic design of the turbine device and Fig. 2 illustrates the exploded view with the acrylic plates omitted. There are three flow paths, which are for rotor driving, static journal air bearing and thrust air bearing, respectively. The 3rd wafer provides a platen for bottom-side dynamic thrust air bearing and the flow paths for driving air as well as for static air bearings. The blades profile for both the rotor and stator are fabricated from the 2nd wafer. The 1st wafer provides the air outlet and a platen for topside dynamic thrust air bearing.

Silicon wafers of 0.4 mm thick are used for 1st and 3rd layers of wafers. A wafer of 0.8 mm thick is used for the 2nd wafer, from which both the rotor and stator are

 ISBN: 2-916187-03-0

fabricated. The rotor has 17 blades with outer and inner diameters of 8.2 mm and 4.4 mm, respectively. The stator has 23 blades as guide vanes. The blade height is designed to be half of the wafer thickness.

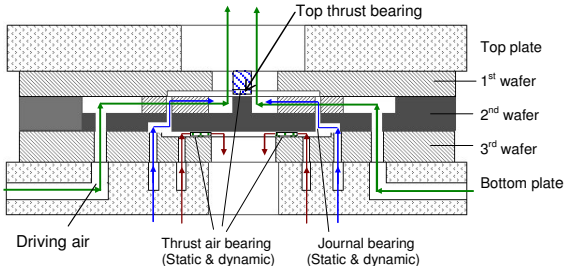

Fig.1 The schematic diagram of the micro turbine device. Three flow paths are for driving air, static journal bearing and static thrust bearing. The dynamic thrust bearings are designed on the 1st and 3rd wafer dies.

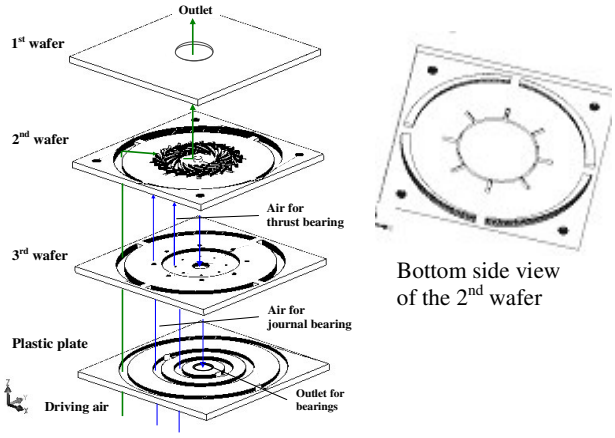

Fig. 2 The exploded view showing the air paths. The bottom-side view of the 2nd wafer shows the slots for static journal bearing

3. DESIGN OF DYNAMIC AIR BEARINGS

3.1. Governing equations

The investigations on micro air bearings are performed based on numerical simulation. The governing equation for dynamic air bearings is Reynolds equation [8].

$$\frac{\partial}{\partial x}(ph^3\frac{\partial p}{\partial x})+\frac{\partial}{\partial z}(ph^3\frac{\partial p}{\partial z}) = 6R\mu\omega\frac{\partial(ph)}{\partial x}+12\mu\frac{\partial(ph)}{\partial t} \quad (1)$$

where h is fluid film height; μ is the viscosity of fluid; and p is the pressure.

$$h = C(1+\varepsilon\cos\theta)+g(x,z) \quad \text{for journal bearing} \quad (2.1)$$

$$h = C+g(x,z) \quad \text{for thrust bearing} \quad (2.2)$$

$$\text{and} \quad g(x,z)=\begin{cases} h_g & \text{in groove region} \\ 0 & \text{on ridge region} \end{cases} \quad (3)$$

The boundary conditions are:

$$p = p_a, \text{at } z=0, z=l \;\&\; r=r_i, r=r_e \quad (4.1)$$

$$p(\theta) = p(\theta+2\pi) \quad (4.2)$$

where p is pressure; h, fluid film height; R, radius; μ, viscosity; ω, angular speed; C, bearing clearance; ε, eccentricity ratio; h_g, groove depth, p_a, ambient pressure, l, journal bearing length; r_i, r_e, inner and outer radius of thrust bearing, respectively.

With the above boundary conditions, Eq. (1) can be solved to obtain the pressure distribution and other dynamic parameters. A commercial software "ARMD 5.4" plus some codes developed on Matlab were used to execute the simulation.

3.2. Design of micro journal bearing

Due to the limitation of manufacturing process, the length of journal bearing (L) is set to one half of wafer thickness, i.e. 0.4 mm. Considering the effective diameter of rotor (D) is 8.28 mm, the aspect ratio of L/D (L/D =0.0483) is extremely low. The load capacity of a plain journal bearing is investigated by employing the above-expressed solutions [9]. Fig. 3(a) shows the simulation results of non-dimensional load capacity $\overline{W}$ versus rotor radii at the aspect ratio of L/D = 0.0483. In the results,

$$\overline{W} = W/W_0 \quad (5.1)$$

$$W_0 = DLp_a \quad (5.2)$$

Where p_a = 1.0135x10^5 Pa, ε in Fig. 3(a) stands for the ratio of bearing eccentricity e versus bearing clearance C (ε=e/C). The load capacity of the journal bearing will increase with the increase of radius of the journal bearing. At the same rotor radius, higher load capacity can also be obtained by reducing the radial clearance C of the journal bearing, as shown in Fig. 3(b). The radial clearance of a journal bearing is defined by the width of a trench between the rotor and stator. A trench of 20 μm wide and 400 μm deep with an aspect ratio of 20 was set in our design.

3.3. Design of micro thrust bearings

The dynamic characteristics of self-acting thrust air bearings in double-side configuration are investigated. Based on the actual turbine structure, a pump-in configuration with spiral grooves is designed for top thrust air bearing, and a pump-out configuration is for bottom bearing, as shown in Figs.4 (a)-(c). Due to the miniaturized dimension and small weight of thrust plate, the axial load is mainly caused by the pressure difference between the top and bottom thrust air bearings.

 ISBN: 2-916187-03-0

Some parameters, such as outer radius R_o, inner radius R_i and groove radius R_m, of a spiral grooves are determined by the turbine dimension and structure. Other parameters that affect the load capacity are investigated. These parameters include groove numbers N_g, groove angle α, axial clearance A_c, groove depth g_d, and groove width ratio a_g (a_g = groove width/(groove pitch)). The axial clearance A_c is the film height on the ridge region of thrust bearing, as shown in Fig. 4(c), and groove depth ratio G_d ($G_d=g_d/A_c$) is adopted in the investigation.

The load carrying capacity and stiffness are investigated based on an assumed rotating speed of 100,000 rpm. If rotation speed increases, the load capacity and stiffness will also increase almost linearly with the increase of the speed.

Fig. 5 shows that load capacity versus groove numbers (N_g) of thrust bearing. The non-dimensional load capacity $\overline{W}$ is defined as $\overline{W} = W / W_0$, and

$$W_0 = \frac{\mu\omega\, r_o^4}{A_c^2} \qquad (6)$$

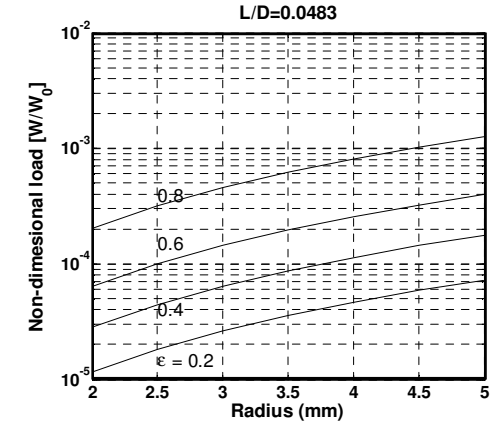

(a) Load capacity versus bearing radius (D/2)

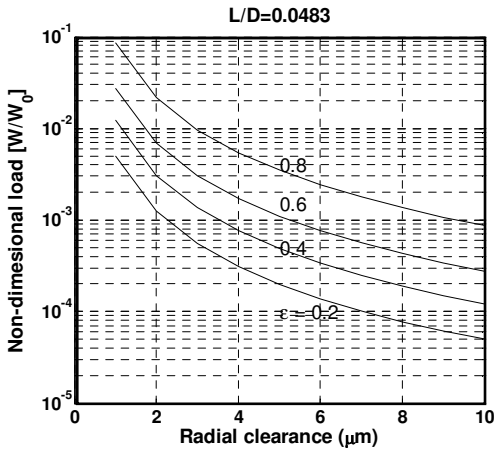

(b) Load capacity versus radial clearance

Fig. 3 Load capacity of a journal bearing

Where ω stands for rotation speed, and μ for dynamic viscosity of air with $\mu = 18.1\times10^{-6}$ Pa s at 20 °C, A_c for axial clearance with A_c = 10 μm in the simulation. It can be seen from Fig. 5 that the load capacity increases with the increase of groove numbers. The effect of groove angle on the load capacity is shown in Fig. 6. It is observed that with the increase of the groove numbers, the peak values of the load capacity gradually move to higher values of groove angles. The investigation on the effect of groove width ratio illustrates that the maximum load capacity can be obtained when the groove width ratio (a_g) ranges from 0.5 to 0.7, provided that the groove numbers are between 6 and 50.

Table 1 illustrates the parameters of dynamic thrust bearings fabricated for the turbine device.

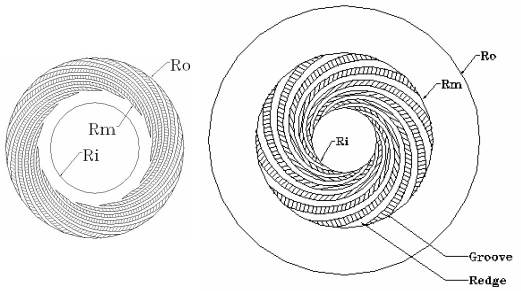

(a) Top thrust bearing (b) Bottom thrust bearing

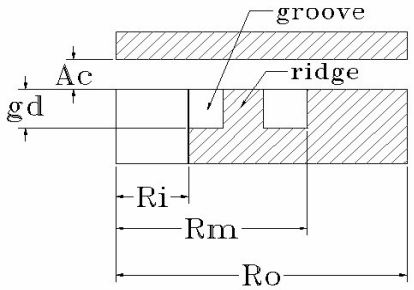

(c) The cross-sectional view of bottom thrust bearing

Fig.4 Schematic views of thrust air bearings consisting of spiral grooves. A_c stands for the axial clearance, g_d for groove depth.

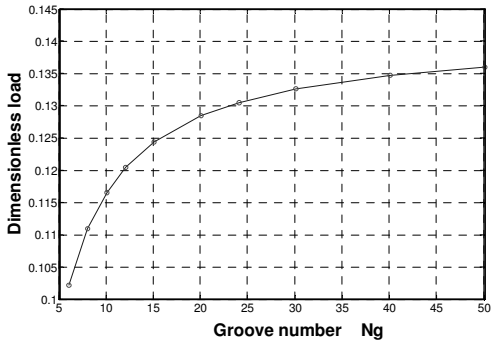

Fig.5 Dynamic load capacity versus groove numbers of a thrust bearing with pump-in configuration

 ISBN: 2-916187-03-0

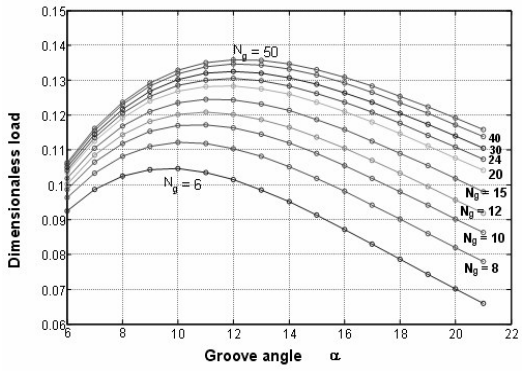

Fig.6 Load capacity versus groove angles of a thrust bearing with pump-in configuration

Table 1: The recommended parameters for top- and bottom- thrust air bearings

	Top thrust bearing	Bottom thrust bearing
Groove pattern	pump-in	pump-out
Outer radius	R_{o1} = 0.9 mm	R_{o2} = 2.6 mm
Middle radius	$R_{m1} = R_{i1}$	R_{m2}= 2.18mm
Inner radius	R_{i1}= 0.36 mm	R_{i2}=1.0 mm
Groove number	N_{g1} = 40	N_{g2} = 40
Groove angle	α_1 = 17.2º	α_2 =19.5º
Groove width ratio	A_{g1} = 0.6	A_{g2} = 0.72
Groove depth ratio	G_{d1} = 3.0	G_{d2} = 3.6

3. FABRICATION

The DRIE (Deep Reactive Ion Etch) process based on inductively coupled plasma is used for fabricating the turbine device. Key process parameters including plasma source power, bias power and process pressure have been optimized to realize high aspect ratio etching with straight sidewalls.

In the 1st wafer, the top thrust bearing using pump-in spiral grooves is first fabricated from the bottom-side surface, followed by through-etching from topside. Since the rotor will be supported by top- and bottom- thrust air bearings, the total axial clearance A_c will be shared by clearance A_{ct} (clearance between rotor and top thrust bearing) and A_{cb} (clearance between rotor and bottom bearing). The design value of total clearance A_c is 15 μm with A_{ct} and A_{cb} being 5 μm and 10 μm, respectively. Hence, the etching depths of grooves for the top- and bottom- bearings are 15 μm and 36 μm, respectively.

In the 2nd wafer, DRIE process is executed from the top to generate the blade profiles of turbine, followed by DRIE etching from bottom to define the high aspect ratio trench between the rotor and stator. The trench functions as the clearance of journal bearing. Fig. 7 shows the top- and bottom- views of the 2nd wafer. A clearance of 20 μm with an aspect ratio of 20 is achieved. The surface roughness of the journal bearing is evaluated by measuring the inner sidewall of stator and outer sidewall of rotor using a Zygo® interferometer. The results show that surface roughness is less than 0.2 μm.

In the 3rd wafer, the bottom thrust bearing using pump-out spiral grooves is fabricated from the top of wafer, followed by DRIE through-etching from the other side. Figs. 8 and 9 show the fabricated thrust bearings. The rotor of the turbine rotates in clockwise direction relative to top bearing while in anti-clockwise direction relative to the bottom bearing.

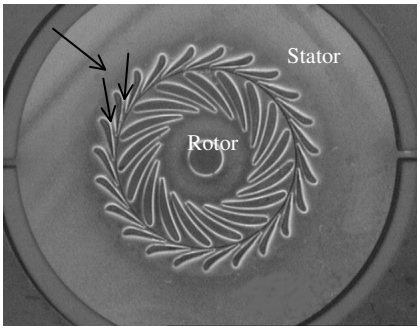

(a) Topside view of the fabricated 2nd wafer

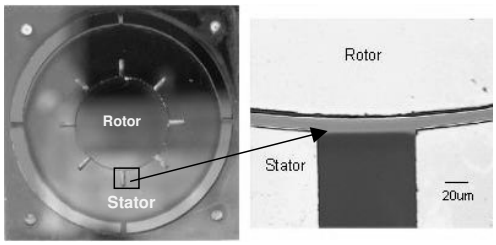

(b) bottom-side view of the fabricated 2nd wafer

Fig.7 The 2nd wafer fabricated using DRIE process

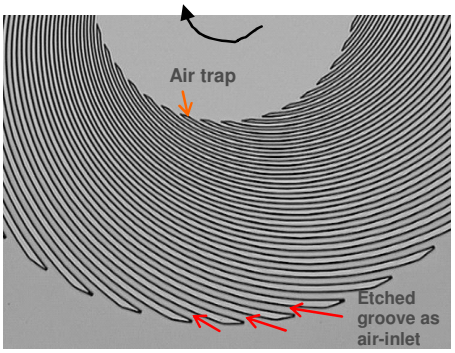

Fig.8 Pump-in spirals for top dynamic thrust bearing with a etch depth of 15 μm. When the rotor rotates in a clockwise direction, air is pumped in via the groove and is trapped in the central area of the bearing.

 ISBN: 2-916187-03-0

5. INTEGRATION AND TESTING

The performance of micro air bearings has been evaluated by measuring the rotation speed of the fabricated micro turbine device. The micro turbine is mounted in an acrylic rig, and then connected to an air distribution system, which consists of the compressed air source, pressure transducers, valve regulators and mass flow meters. Fig.10 shows the experimental setup. An optical fiber sensor is used to monitor the rotation of the micro turbine.

Fig. 11 demonstrates the real time output signal of the optical fiber sensor, which shows that the rotational speed is 3516 rpm when the flow rate of compressed air is 7.2 slpm (standard liter per minute). The signal from the fiber sensor can also be used for Fast Fourier Transform (FFT) to calculate the rotational speed and stability. Fig. 12 demonstrates one example. The spectrum analysis based on FFT indicates that the rotation speed is relatively uniform during operation while the flow rate is being kept constant. Stable operations of 15,000 rpm have been achieved during testing.

6. CONCLUSION

We have developed a silicon-based micro turbine device, which consists of both journal bearing and thrust air bearings with parameters recommended by simulation. The characteristics and performances of micro air bearings are studied through numerical simulation. It is found that the load capacity of a micro journal bearing with low aspect ratio (L/D=0.0483) will increase with rotor diameter, and almost linearly increase with the bearing number (rotation speed). Higher load capacity can be achieved by increasing the value of *L/D* or decreasing the radial clearance of a journal bearing.

The investigations on the dynamic thrust bearings demonstrate that the load capacity of thrust bearing increases with groove numbers. With the increase of the groove numbers, the peak values of the load capacity gradually move to higher values of the groove angle. A silicon-based micro turbine device has been designed and fabricated. A micro journal bearing with aspect ratio above 20:1 is realized using optimized DRIE process. Experimental tests demonstrate that the turbine device can sustain stable operations, and a rotation speed of 15,000 rpm has been achieved.

ACKNOWLEDGEMENTS

The authors would like to thank SIMTech and the Agency for Science, Technology and Research (A*Star), Singapore for the project funding.

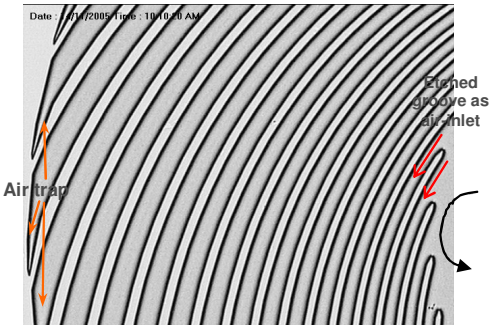

Fig. 9 Pump-out spirals for bottom bearing. Air is pumped out while rotor relatively rotates in anti-clockwise direction

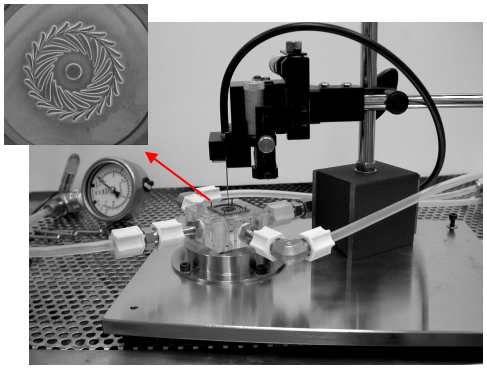

Fig. 10 The setup for testing the developed turbine device

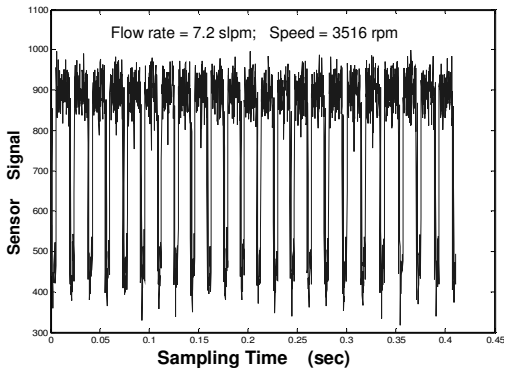

Fig. 11 Output signal of fiber sensor

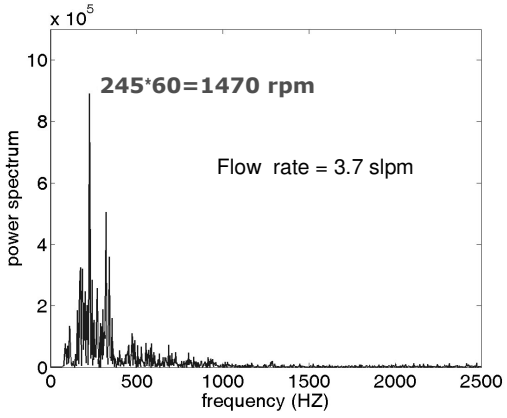

Fig. 12 FFT analysis of signal from the fiber sensor

 ISBN: 2-916187-03-0

REFERENCES

[1] A. H. Epstein, "Millimeter-scale MEMS gas turbine engines", *Proc. of ASME Turbo Expo2003 -Power for Land, Sea and Air*, USA, Vol. 1**,** pp. 1-28, 2003.

[2] K. Isomura, S. Tanaka, S. Togo, H. Kanebako, M. Murayama, N. Saji, F. Sato and M. Esashi, "Development of micromachined gas turbine engine for portable power generation", *JSME Internationa Journal Series B,* Vol.47, pp.459-464, 2004.

[3] X C Shan, Z F Wang, Y F Jin, M Wu, J Hua, C K Wong and R Maeda, "Studies on a micro combustor for gas turbine engines", *J. Micromech. Microeng,* Vol. 15, S215–S221, 2005.

[4] S. Tanaka, K. Isomura, S. Togo and M. Esashi, Turbo test rig with hydro-inertia air bearings for a palmtop gas turbine, *J. Micromech. Microeng*. Vol.14, pp.1449-1454, 2004.

[5] M. Hara, S. Tanaka and M. Esashi, "Infrared polarization modulator using a MEMS-based air turbine", *J. Micromech. Microeng,* Vol.13, pp. 223-228, 2003.

[6] L.G. Frechette, S.A. Jacoson, et al, "Demonstration of a microfabricated high-speed turbine supported on gas bearings", *Proc. of Solid-State Sensor and Actuator Workshop*, Hilton Head Island, pp.43-47, 2000.

[7] E. S. Piekos, "Numerical simulation of gas-lubricated journal bearings for micro-fabricated machines", *Doctoral thesis,* MIT, 2000.

[8] J. Hamrock, *Fundamentals of fluid lubrication*, McGraw-Hill, Inc., New York, 1994.

[9] Q. D. Zhang, X.C. Shan, G. Guo and C. K. Wong, "Performance Analysis of Air Bearing in a Micro System", to be published in *J. of Materials Science and Engineering A*.

 ISBN: 2-916187-03-0